14th International Conference on Structural Safety and Reliability - ICOSSAR'25
1-6 June, 2025 - Los Angeles California, USA

A FRAMEWORK FOR THE REDUCTION OF WIND-INTENSIFIED WILDFIRES CAUSED BY FAILURES IN POWER DISTRIBUTION SYSTEMS

AMIR TAJIK [1] AND YOUSEF DARESTANI [2]

[1] Michigan Technological University
Dow 852, 1400 Townsend Dr, Houghton, MI 49931
Tajik@mtu.edu

[2] Michigan Technological University
Dow 811, 1400 Townsend Dr, Houghton, MI 49931
ydaresta@mtu.edu

Key words: Wildfire, Power system fragility, Wind seasonality, Sequential Monte Carlo, Structural risk mitigation, Fallen trees

Abstract. *In Southern California, hot and dry seasonal weather effects such as Santa Ana winds are major wildfire drivers. Such events not only make vegetation dry, creating fuel for wildfires, but they also inflict damage to power system equipment, causing conductors to fall on the ground resulting in sparks and excessive heat that may ignite wildfires. The existing literature on this subject reveals several limitations that have not been properly addressed. No study provides seasonal hazard models for hot and dry wind events in the current literature. There is also a notable gap in models that estimate the probability of fire ignition due to wind-induced failures in power system components, particularly those associated with fallen trees. Lastly, there is a lack of a probabilistic model for the degradation of power system components against fire, especially for wood poles. This study develops a comprehensive framework to assess and mitigate wildfire risks to power systems. The framework first develops a joint probability distribution based on the maximum monthly wind speeds and integrates them through a sequential Monte Carlo process to predict wind events. Second, wildfire ignition probability due to power system failures, incorporating physics-based models for tree failures, conductor impacts, and vegetation ignition is developed. Third, a probabilistic wildfire progression model that considers various factors influencing fire behavior and its effects on power systems is developed. Finally, the framework investigates the impact of wildfire on wood poles through a heat transfer analysis and estimation of charring. Results indicate that the frequency of wildfire incidents and the resulting extent of damage can be substantially reduced through strategic tree density management. This study offers utility managers and regulators a framework for improving the power system components' risk to fire exposure.*

1 INTRODUCTION

In the past few decades, the United States has experienced a rising trend in wildfire incidents. This could be attributed to climate change, increase in dead vegetation fuel, and accelerated urbanization [1]. Wildfires could be triggered from natural phenomenon such as lightning or human intervention such as campfires, or as a result of power system equipment failures.

Among these, wildfires triggered by failure in power systems are the only category of fire hazards that are triggered and amplified by wind events. California frequently experiences seasonal hot and dry winds (Santa Ana and Diablo winds), which dry out vegetation and can damage power infrastructure with gusts reaching over 80 miles per hour [2, 3]. Although power system failures cause only 1% of Southern California wildfires, they contribute to more than 10% of the area burned. This is seen in the devastating 2018 Camp Fire, which was initiated by failure in the transmission system [4, 5]. Among all failure modes in power systems, the failure caused by fallen trees is a dominant cause of wildfires, as trees can easily fall over in normal wind conditions. Fallen trees may fall over conductors, and break them, potentially causing a short circuit that could produce a significant amount of heat, drying ground vegetation and igniting wildfires.

The existing literature does not offer a comprehensive analysis of the impact of hot and dry wind events in initiating wildfires. This is primarily due to the complexities associated with wind events, system failures, and fire ignition and propagation. Current wind hazard modeling methods; including the annual maxima, Peak-Over-Threshold, and Poisson Point Process; do not adequately capture the seasonality and temporal correlations in consecutive events [6] such as Santa Ana and Diablo winds. It is critical to point out that such events can occur multiple times within a month or a year [7, 8]. Additionally, despite numerous efforts in developing wind fragility functions for utility poles [9, 10], the fragility models for conductor breakage due to windthrown fallen trees are significantly underdeveloped. Such models [11, 12] often oversimplify the interaction of fallen trees and conductors by neglecting dynamic impact loads from falling trees [13]. Wildfire ignition from power system failures can lead to flaming combustion. However, to this date, there is no model to predict the probability of fire ignitions under tree-induced failure conditions. Data-driven models derived from experiments or field data may not be suitable as they are always only applicable to local conditions, and other physics-based efforts are also significantly underdeveloped [14, 15]. To address these knowledge gaps, this paper proposes a novel framework integrating physics-based and data-driven models to estimate wildfire risks as a result of failure in power systems. The framework develops new wind models to account for seasonal hot-dry wind events and integrates them with dynamic analysis of tree conductor interaction to investigate conductor breakage. These models will be combined with ignition and fire propagation models to estimate the risk imposed on a real distribution network in Southern California.

2 FAILURE ANALYSIS

The probability of failure for a structural system depends on a set of parameters including the hazard intensity measures and deterministic and probabilistic (uncertain) structural and non-structural parameters [16, 17]. Fragility models were first developed to estimate the probability of failure conditioned on the hazard intensity. It should be noted that in risk analysis, the uncertainties in hazard intensity will be accounted for when the fragility model is integrated with the hazard model. Therefore, when developing fragility models, hazard intensity measures are assumed to be deterministic parameters. Furthermore, while some structural and non-structural parameters, such as the tensile capacity of conductors, are uncertain in nature, other parameters, such as the length of the conductor, can be easily determined for a particular conductor. Therefore, such parameters could be assumed to be deterministic. The concept of

parametrized fragility functions was developed to address this challenge [16]. Parametrized fragility functions provide a simple yet accurate function that estimates failure probability conditioned on both hazard intensity and structural and non-structural parameters. In this study, a parametrized fragility function that accounts for the breakage of conductors under wind-thrown fallen trees is developed. Such a fragility model will be later used in conjunction with data-driven fire ignition models to estimate the risk associated with wildfires triggered by wind-related failures in power system equipment.

3 FRAGILITY OF CONDUCTORS UNDER WIND-THROWN FALLEN TREES

A logistic regression method is used in this study to develop a parameterized fragility model for conductors affected by windthrown fallen trees. To develop the fragility model, numerous samples of intensity measures and characteristics of trees and conductors are generated using Halton quasi-random point sets [18]. Additionally, uncertain parameters are sampled through the Latin Hypercube Sampling (LHS) technique [19]. In the following the framework to apply logistic regression is explained.

3.1 Failure of trees under wind load

In strong wind gusts, trees may either break at the trunk or may uproot (Peltola 2006). Uprooting occurs when the wind-induced overturning moment at the groundline exceeds the resisting moment provided by the root-soil anchorage. This wind-induced moment can be calculated using the wind model from ASCE7 [20]. For a non-building structure, the wind force per unit length is calculated as:

$$f_{wind}(z) = q_z(z) G C_f(z) D(z) \tag{1}$$

where C_f is the wind force coefficient, G is the gust factor, and q_z is the velocity pressure. D is the surface diameter of trees. The ASCE 7 [20] outlines the calculation methods for each of these parameters. In Eq.(1), some of the parameters are uncertain. As noted earlier, uncertain parameters for generating samples in logistic regression are obtained using an LHS method [9]. Additional parameters, are treated as deterministic inputs to the fragility model. These parameters are created using a Halton quasi-random point set. The moment demand at the groundline can be estimated by applying Eq. (1) to a tree and computing it over its height:

$$M_s = \int_{H_t - H_{Cr}}^{H_t} f_{wind_C}(z).z.dz + \int_0^{H_t} f_{wind_s}(z).z.dz \tag{2}$$

where H_{Cr} is the height of the crown; $f_{wind_C}(z)$ is the wind per unit length on the crown obtained from Eq.(1); $f_{wind_s}(z)$ is the wind force per unit length on the tree's stem obtained using Eq.(1), H_t is the tree's height, and z is the ground line elevation. The resisting moment preventing uprooting can be estimated using [21]:

$$M_{R-Uproot} = c_{reg}\, \rho_s V_s \tag{3}$$

where c_{reg} is the regression constant obtained by tree-pulling experiments and varies with tree species, ρ_s is the density of the tree's stem, and V_s is the volume of the tree's stem. When M_s exceeds $M_{R-Uproot}$, the tree fails under the uproot mechanism. Stem breakage (snapping) may

occur when wind-induced compressive stress, σ_S, exceeds the modulus of rupture of the tree's stem, σ_R. σ_S can be determined as

$$\sigma_S = \frac{M_{z_b} D_s(z_b)}{2I_{z_b}} + \frac{W_{tr,z_b}}{A_{z_b}} \tag{4}$$

where M_z, D_s, I_z, and A_{z_b} are respectively the wind induced moment, the diameter of the stem, the moment of inertia, and the cross-sectional area of the stem, all at the elevation z_b, the breakage elevation. W_{tr,z_b} represents the weight of the tree above elevation z_b.

3.2 Tree falling on conductors

This study assumes that the fallen tree performs as an inverted pendulum, with the breakage point modeled as a hinge. The tree falls freely in line with the wind angle, as shown in Fig. 1. The tree hits the conductor if the following equation is satisfied:

$$H_t \geq \frac{\sqrt{(z_c(y_{hit}) - z_b).cos^2(\alpha) + \left(d_{tc} - d_{hp}\right)^2}}{cos(\alpha)} + z_b \tag{5}$$

where H_t is the tree height; d_{tc} is the distance between the tree and the closest; d_{hp} is the horizontal spacing between the side and central phase conductors; z_b represents the tree's failure elevation; and α is the wind angle measured from the x-axis and ranges from -90 to 90 degrees. z_c is the elevation of conductors at any given point along the span computed via Eq. (6), assuming a parabolic form for the conductor under its own weight [22].

$$z_c(y) = 4\psi\left(\frac{y - d_{off}}{l_{span}}\right)^2 + h_{pole} - d_{vp} - \psi; \quad d_{off} - \frac{l_{span}}{2} \leq y \leq d_{off} + \frac{l_{span}}{2} \tag{6}$$

where d_{off} is the offset from the middle of the span; l_{span} is the span length; h_{pole} is the height of the pole; d_{vp} is the vertical spacing between the side and central phase conductors; and ψ is the sag at midspan and computable via the following equation:

$$\psi = \frac{w_c l_{span}^2}{8T_{c0}} \tag{7}$$

where T_{c0} is the pre-tensioning force and w_c is the unit weight of conductors [22]. y_{hit} is the potential point of contact and is estimated from the following equation:

$$y_{hit} = \left(d_{tc} - d_{hp}\right) tan(\alpha) \tag{8}$$

If the wind angle is excessively wide, the tree could bypass either side of the span of interest. Consequently, the tree would only impact the span of interest if $\alpha_1 \leq \alpha \leq \alpha_2$. α_1 and α_2 can be determined using the following equation:

$$\alpha_1 = arctan\left(\frac{d_{off} - \frac{l_{span}}{2}}{d_{tc}}\right), \; \alpha_2 = arctan\left(\frac{d_{off} + \frac{l_{span}}{2}}{d_{tc}}\right) \tag{9}$$

where d_{off} is the offset, i.e. the distance of the tree from the middle of the span in direction y (the axis parallel to the span in Fig. 1).

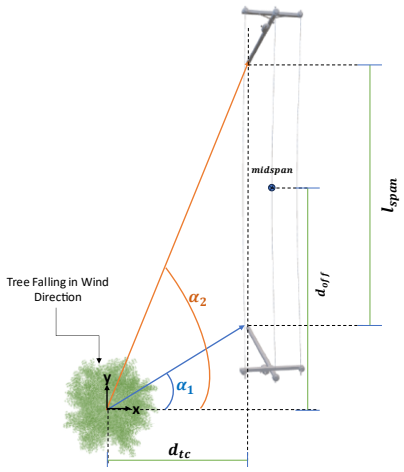

Figure 1: Geometric arrangement of the tree and span prior to contact. It is assumed that the tree falls in the direction of the wind.

3.3 Conductor failure

For cases where the tree fails and the conductor is positioned such that the fallen tree would hit the conductor, the dynamic interaction between the fallen tree and the conductor is modeled in LS-DYNA R10.1.0. [23]. The tree is modeled as an inverted pendulum with a starting tangent angle of 5%. The conductor is modeled as an elastic cable material lacking compression capacity using MAT_071: CABLE_DISCRETE_BEAM in LS-DYNA. A bilinear stress-strain curve is also included to represent plastic behavior of the conductor. It is assumed that the conductors are pinned at both ends. When the tree falls on the conductors, it exerts an impact load. The maximum tensile force experienced by the conductor is compared against its ultimate tensile capacity. The conductor is classified as a failed member if the tensile force surpasses this limit. Following this, binary outputs are generated for logistic regression analysis.

3.4 Fragility models

In this study, logistic regression is employed to develop fragility models of ACSR conductors subjected to wind-driven fallen ponderosa pines in three-phase distribution networks. The data on 19 types of ACSR conductors with two different aluminum-to-steel standing ratios, 6 to1 and 26 to 7 is collected from industrial catalogs [24]. The conductors' diameter ranges from 5 to 28.1 millimeters. Using conductor, trees, and wind data, 100,000 samples of uncertain and deterministic features are generated using Halton quasi-random point set and LHS methods. These samples will be used to train for logistic regression analysis. The logistic regression will be trained based on a binary target variable indicating failure/survival from the following sequence of events:

$$E_{cf} = E_{tf}.E_{tc}.E_{cb} \tag{10}$$

where E_{tf} is binary variable representing the event of failure of the tree; E_{tc} is the event of tree hitting the conductor given the tree failure; E_{cb} is the event of conductor breakage given the tree has already failed and hit the conductor. The fragility model for ACSR conductors due to a stem breakage has the following form:

$$P_{cf,sb}\left(v,\alpha,h_t,h_p,d_{tc},l_s,d_{off},D_c\right)=$$
$$\begin{cases}\dfrac{1}{1+e^{-L_s\left(v,\alpha,h_t,h_p,d_{tc},l_s,d_{off},D_c\right)}}, & d_{tc}\le h_t.cos(\alpha)\ and\ \alpha_1\le\alpha\le\alpha_2\\ 0, & d_{tc}\ge h_t.cos(\alpha)\ or\ \alpha\notin[\alpha_1,\alpha_2]\end{cases} \tag{11}$$

where L_s is determined as

$$L_s\left(v,\alpha,h_t,h_p,d_{tc},l_s,d_{off},D_c\right)=$$
$$a_0+a_1.v.h_t.H\left(h_t-h_p\right)+a_2.\frac{v^2}{h_t.D_c}\left(h_t^2.cos^2(\alpha)-h_p^2.cos^2(\alpha)-d_{tc}^2\right)+a_3.\left(\frac{v}{h_t}\right)^{\frac{3}{2}}\left(\frac{l_s}{2}-d_{off}\right) \tag{12}$$

where $H(x)$ is the Heaviside step function. Additionally, the failure probability of ACSR conductors for uproot mechanism is estimated by the following set of equations forming the fragility model:

$$P_{cf,up}\left(v,\alpha,h_t,h_p,d_{tc},l_s,d_{off},D_c\right)=P_{up}(v,h_t).P_{cf_0}\left(\alpha,h_t,h_p,d_{tc},l_s,d_{off},D_c\right) \tag{13}$$

$$P_{up}(v,h_t)=\frac{1}{1+e^{-L_u\left(v,h_t\right)}} \tag{14}$$

$$L_u(v,h_t)=c_0+c_1h_t+c_2v \tag{15}$$

$$P_{cf_0}\left(\alpha,h_t,h_p,d_{tc},l_s,d_{off},D_c\right)=$$
$$\begin{cases}\dfrac{1}{1+e^{-L_0\left(\alpha,h_t,h_p,d_{tc},l_s,d_{off},D_c\right)}}, & d_{tc}\le h_t.cos(\alpha)\ and\ \alpha\in[\alpha_1,\alpha_2]\\ 0, & d_{tc}\ge h_t.cos(\alpha)\ or\ \alpha\notin[\alpha_1,\alpha_2]\end{cases} \tag{16}$$

$$L_0\left(\alpha,h_t,h_p,d_{tc},l_s,d_{off},D_c\right)=$$
$$b_0+b_1.H\left(h_t-h_p\right)+b_2.\frac{1}{h_t^2.D_c}.\left(h_t^2.cos^2(\alpha)-h_p^2.cos^2(\alpha)-d_{tc}^2\right)+b_3.h_t.\left(\frac{l_s}{2}-d_{off}\right) \tag{17}$$

The regression coefficients for both fragility models are presented in Table 1. The AUC scores for the test dataset exceed 0.97, suggesting that the logistic regression model performs effectively with the chosen design variables.

Table 1. Regression coefficient for the fragility functions

Failure mode:	Stem-breakage-induced Cable Failure				Uproot-induced Cable Failure						
AUC Score	0.977				0.977						
Coefficients:	a_0	a_1	a_2	a_3	b_0	b_1	b_2	b_3	c_0	c_1	c_2
Value:	-6.900	1.27E-03	1.13E-07	5.33E-03	-6.937	4.249	0.055	0.00276	-18.155	0.1668	0.1669
P-value:	0	0	0	0	7.3E-54	3.2E-21	0	0	0	0	0

A numerical study was performed to demonstrate how the fragility of conductors varies with wind speed, conductor's diameter, and tree's height. Fig 2. shows the likelihood of conductor failure increases with the increase in tree's height and decrease in conductor's diameter.

4 FIRE IGNITION AND IMPACT MODELING

So far, fragility models have been developed for tree-driven failure of conductors under wind events. In this stage, models will be developed to address the vegetation ignitions followed by fallen conductors, the potential wildfire spread, and the subsequent degradation of the wood

poles. These models will be used in combination with the fragility models to estimate the frequency of expected wildfire hazard and degradation of poles.

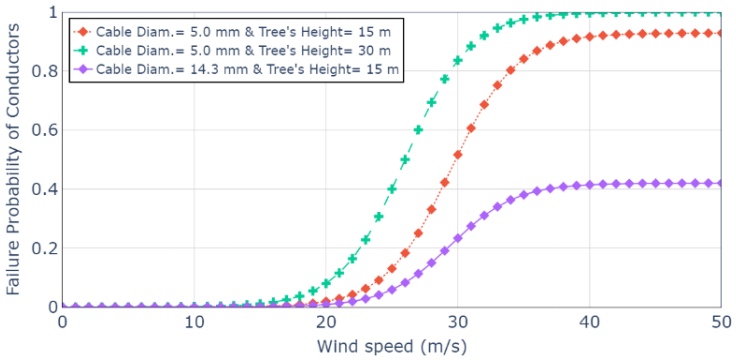

Figure 2: Effects of cable's diameter and tree's height on fragility curves of conductors if hit by an uprooted ponderosa pine. Other parameters fixed at $\boldsymbol{\alpha = 0}$, $\boldsymbol{h_{pole} = 11\ m}$, $\boldsymbol{d_{tc} = 5}$ m, $\boldsymbol{d_{off} = 0}$, and $\boldsymbol{l_{span}} = 40$ m.

4.1 Probability of vegetation ignition

In this study, the focus is on the flaming combustions as they spread much faster and more violently, and therefore, much more difficult to suppress. The data-driven model proposed by the National Wildfire Coordinating Group [25] is used to estimate the likelihood of sustained ignition in the dried vegetation when exposed to the electrical arc of a downed conductor. This model predicts ignition probabilities as a function of moisture in dead vegetation, the season, and the slope of the study area.

4.2 Fire Progression Model

For those ignitions resulting in widespread fires, Rothermel's surface fire spread is employed to simulate wildfire progression [26]. The model is a physics-based approach based on standard fuel parameters [27]. This model estimates the rate of spread (m/s) of the flaming front by

$$R = \frac{I_R \xi (1 + \phi_w + \phi_s)}{\rho_b \varepsilon Q_{ig}} \tag{18}$$

where I_R is reaction intensity (J/m²·s), the rate of energy release per unit area; ξ the propagating flux ratio, the fraction of energy that preheats unburned fuel; ϕ_w and ϕ_s the wind and slope factors, respectively; ρ_b the bulk density of the fuel bed (kg/m³), ε the effective heating number, the fraction of fuel heated to ignition, and Q_{ig} the heat of preignition (J/kg). Based on the estimated spread rate, the model follows an elliptical fire propagation pattern with the ignition point as the focal point. The model accounts for wind speed, direction, and terrain slope and tracks the perimeter expansion over time. [26]. The rate of spread for the points on ellipse can be adjusted based on the angle ψ they make with the ignition point. The model calculates the fireline intensity (w/m) in different points by

$$I_B(\psi) = H_A R_\psi \tag{19}$$

where R_ψ is the rate of spread at angle ψ, and H_A the heat per unit area (J/m²). Flame height F_H

in meters at any point on fireline is estimated using Byram's empirical relation [26]:

$$F_H(\psi) = 0.00323 I_B^{0.46}(\psi) \tag{20}$$

4.3 Pole structural degradation

To assess the impact of wildfire on the wood poles, the thermal exposure needs to be calculated. Therefore, the fire perimeter at each time t is divided into multiple flame elements, and the total radiative heat flux is estimated by summing the contribution from each element as follows:

$$q(t) = \sum_{i=1}^{N} \epsilon_f \sigma \left(T_f^4 - T_\infty^4\right) V_{f_i} . l_i \tag{21}$$

where ε_f is flame emissivity (0.9), σ Stefan-Boltzmann constant (5.67×10^{-8} W/m²·K⁴), T_f flame temperature (1200 ℃), T_∞ the ambient temperature, and l_i the length of the flamelet. V_{f_i} denotes the view factor of flamelet i at time t computed by

$$V_{f_i} = \frac{h_{f,i}^2}{d_i^2 + h_{f,i}^2} cos\beta_i \tag{22}$$

where h_f is the flame height, d_i the distance between flamelet and the pole, and β the angle between the flamelet's normal vector and line connecting pole and center of the flamelet. It is important to note that this study considers only surface fire spread and radiative heat transfer. Other mechanisms, such as crown fire propagation and convective preheating, are not included. The material degradation of wood poles is quantified using a temperature-dependent charring model that considers material properties, including specific gravity and moisture content [28]:

$$\dot{c} = \left(\frac{1.27}{A}\right) e^{-\frac{JE}{RT_s}}$$
$$A = 7.587 + 0.153m \tag{23}$$

where $\dot{c}$ is charring rate (mm/s), and m the wood pole moisture content dependent on temperature and relative humidity [29]. T_s represents the pole surface temperature (K) calculated from the energy balance:

$$T_s = \sqrt[4]{\left(T_\infty^4 + \frac{q}{\epsilon_w \sigma}\right)} \tag{24}$$

where ϵ_w is wood emissivity. The minimum temperature to activate charring is set based on the onset of wood pyrolysis. $\frac{JE}{R}$ is 1744 K for southern pines. Ultimately, diameter reduction at ground level (ΔD) is estimated by integrating charring over fire exposure duration:

$$\Delta D = 2 \int \dot{c}\,(T_s(t))dt \tag{25}$$

5 SEASONAL WIND HAZARD MODEL

Wind hazard models are typically developed based on annual exceedance probabilities. This study shifts the hazard model from an annual to a monthly basis to consider the unique seasonal

characteristics of Santa Ana and Diablo winds. This model resamples historical events to predict future wind occurrences based on the frequency, timing, and intensity expected each year.

6 SEASONAL WILDFIRE RISK ASSESSMENT

To properly address the various uncertainties within and across years, a Sequential Monte Carlo (SMC) process is employed to estimate the fire ignition probabilities. The process checks the sequence of events when a power distribution span faces seasonally varied winds across months, and considers the possibility of multiple ignitions within a year. This method predicts annual expected ignitions by each power span and subsequent charring of wood poles. The framework follows this workflow for S scenarios and then averages the results: (1) run the seasonal wind hazard model to generate n vectors of wind realizations, including year, month, and gust speed; (2) for each wind event realization, evaluate span failure using the generated fragility models by sampling Bernoulli trials; (3) for the failure cases, assess the occurrence of vegetation ignition based on the availability of dead vegetation and sampled temperature, humidity, and hour of the day; (4) similarly, for the cases of vegetation ignitions, evaluate whether any lead to wildfire spread; (5) ultimately, for the cases of wildfire propagation, estimate the charring of the wood poles.

7 NUMERICAL STUDY

The framework discussed earlier is adopted to assess the wildfire risk in a selected distribution network in Crestline, CA. The power system comprises 81 wood poles. In this distribution network, Pigeon ACSR conductors are supported by 9.3 meters high Class 3 wood poles. It is assumed that there are two rows of ponderosa pine trees on each side of the road. Trees are spaced evenly at 5 m intervals and 5 meters away from the conductors. The road width is assumed to be 10 meters. Additionally, it is assumed that around 10% of the land near the distribution lines is covered by dead vegetation. Average cloud coverage is assumed to be less than 50%. Additionally, winds are predominately northeasterly to replicate the direction of Santa Ana wind events.

To develop a site-specific seasonal hazard model, daily weather data (for more than 24 years) on precipitation and maximum wind gust speeds are collected from a nearby station at Riverside Municipal Airport [30]. The temperature and humidity data from the same station are also collected to estimate the probability of vegetation ignitions. This study assumes that only 5% of the power-system-induced ignitions result in widespread wildfires. The fire spread rate is estimated based on SB2 fuel model, which is assumed to be the best choice due to extensive tree mortality and the presence of dense, downed woody debris and fine surface fuels in the study region [27, 31]. Finally, the ground slope is approximately 30% downward southwest. This data is used to estimate the expected monthly fire incidents for the current system compared with the case where the first row of trees on each side of the road is removed. Results (shown in Fig. 3) indicate that by adopting the tree-cutting strategy, wildfire incidents could decrease from 0.289 to 0.078 per calendar year (73% reduction). Moreover, Fig 4. Presents the impact of tree removal on the reduction in pole diameter as a result of charring effect from wildfires. The results are obtained by performing a sequential Monte Carlo simulation for a period of 50 years. The tree cutting strategy has successfully reduced the maximum degradation in pole diameter from 18% to about 5% (13% improvement). These findings highlight the

importance of tree management plans in areas with significant wildfire risks.

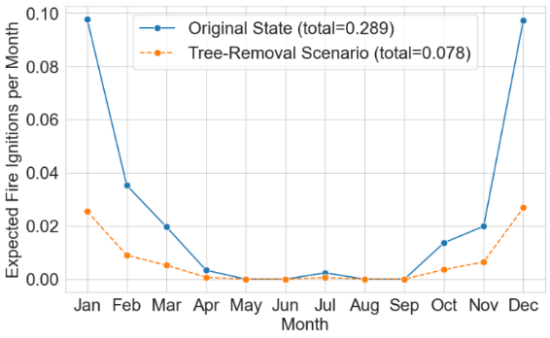

Figure 3: Expected monthly fire ignitions before and after the mitigation scenario.

8 CONCLUSIONS

This study developed a physics-based fragility model for the breakage of conductors subjected to windthrown fallen trees using logistic regression. The fragility model is integrated with a novel seasonal data-driven wind hazard model, creating a comprehensive framework that incorporates fire ignition and propagation models. This framework was employed to estimate the expected number of wildfire incidents and the subsequent degradation of distribution poles in wildfire-prone areas of Southern California. The results indicated that tree removal programs could reduce the expected number of vegetation ignitions near power distribution systems by 73% and the diameter reduction of the vulnerable wood poles by 13%.

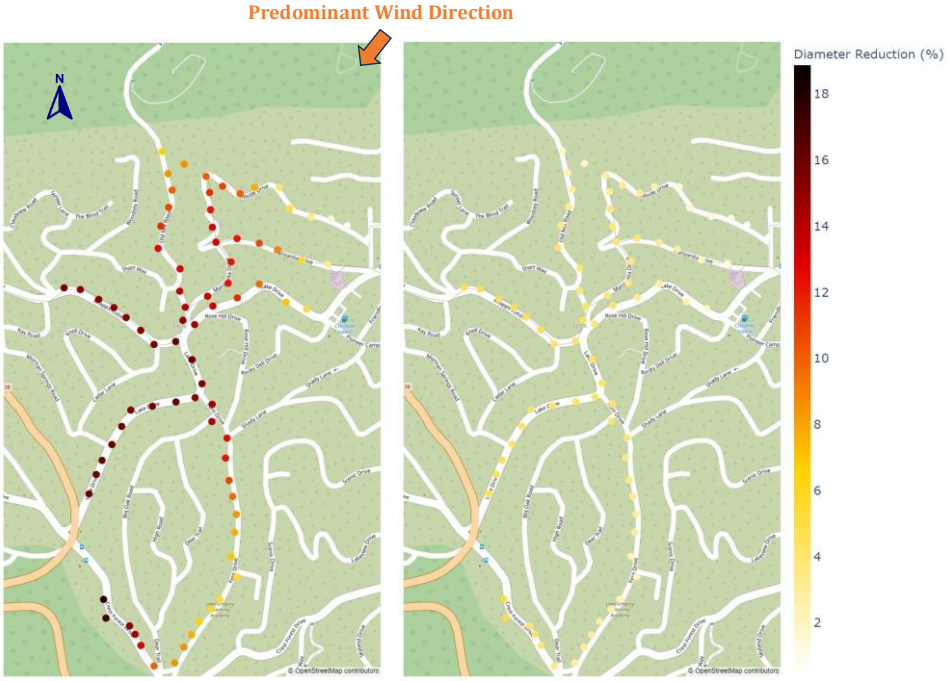

a) Original state b) Tree-removal scenario

Figure 4: Expected diameter loss in 50 years due to charring under wildfires for a) the original state and b) the post-mitigation scenario.

9 REFERENCES

[1] National Interagency Fire Center. Total Wildland Fires and Acres (1983-2022), https://www.nifc.gov/fire-information/statistics/wildfires; 2024 [accessed 03/01/2024.

[2] Raphael M. The santa ana winds of california. Earth Interactions 2003;7(8):1-13.

[3] Fire Weather Research Laboratory. Diablo Winds: California's Critical Fire Weather Pattern, https://www.fireweather.org/diablo-winds; 2025 2025].

[4] Joseph WM. Power line failures and catastrophic wildfires under extreme weather conditions. Engineering Failure Analysis 2013;35:726-35. https://doi.org/https://doi.org/10.1016/j.engfailanal.2013.07.006.

[5] Sayarshad HR. Preignition risk mitigation model for analysis of wildfires caused by electrical power conductors. International Journal of Electrical Power & Energy Systems 2023;153:109353.

[6] Shid-Moosavi S, Di Cioccio F, Haghi R, Tronci EM, Moaveni B, Liberatore S, et al. Modeling and experimentally-driven sensitivity analysis of wake-induced power loss in offshore wind farms: Insights from Block Island Wind Farm. Renewable Energy 2025;241:122126.

[7] Slimacek V, Lindqvist B. Reliability of wind turbines modeled by a Poisson process with covariates, unobserved heterogeneity and seasonality. Wind energy 2016;19(11):1991-2002.

[8] Palutikof JP, Brabson B, Lister DH, Adcock S. A review of methods to calculate extreme wind speeds. Meteorological applications 1999;6(2):119-32.

[9] Darestani YM, Shafieezadeh A. Multi-dimensional wind fragility functions for wood utility poles. Engineering Structures 2019;183:937-48.

[10] Du W-L, Fu X, Li G, Li H-N. An efficient nonlinear method for cascading failure analysis and reliability assessment of power distribution lines under wind hazard. Reliability Engineering & System Safety 2024;245:109995.

[11] Canham CD, Papaik MJ, Latty EF. Interspecific variation in susceptibility to windthrow as a function of tree size and storm severity for northern temperate tree species. Canadian Journal of Forest Research 2001;31(1):1-10.

[12] Hou G, Chen S. Probabilistic modeling of disrupted infrastructures due to fallen trees subjected to extreme winds in urban community. Natural Hazards 2020;102(3):1323-50.

[13] Hou G, Muraleetharan KK. Modeling the Resilience of Power Distribution Systems Subjected to Extreme Winds Considering Tree Failures: An Integrated Framework. International Journal of Disaster Risk Science 2023;14(2):194-208.

[14] Muhs JW, Parvania M, Nguyen HT, Palmer JA. Characterizing probability of wildfire ignition caused by power distribution lines. IEEE Transactions on Power Delivery 2020;36(6):3681-8.

[15] Bayani R, Waseem M, Manshadi SD, Davani H. Quantifying the risk of wildfire ignition by power lines under extreme weather conditions. IEEE Systems Journal 2022;17(1):1024-34.

[16] Darestani Y, Padgett J, Shafieezadeh A. Parametrized Wind–Surge–Wave Fragility Functions for Wood Utility Poles. Journal of Structural Engineering 2022;148(6):04022057. https://doi.org/doi:10.1061/(ASCE)ST.1943-541X.0003319.

[17] Sohrabi S, Darestani Y, Pringle WJ, Dowden DM, Dehghanian P. Life Cycle Cost Analysis of Prestressed Concrete Poles Subjected to Wind, Surges, and Waves. Journal of Structural Engineering 2025;151(7):04025069. https://doi.org/doi:10.1061/JSENDH.STENG-13840.
[18] Kocis L, Whiten WJ. Computational Investigations of Low-Discrepancy Sequences. ACM Trans Math Softw 1997;23(2):266–94 , numpages = 29. https://doi.org/10.1145/264029.264064.
[19] Helton JC, Davis FJ. Latin hypercube sampling and the propagation of uncertainty in analyses of complex systems. Reliability Engineering & System Safety 2003;81(1):23-69. https://doi.org/https://doi.org/10.1016/S0951-8320(03)00058-9.
[20] ASCE. Minimum design loads for buildings and other structures. Standard ASCE/SEI 7-22. Reston, VA, USA; 2022.
[21] Gardiner B, Peltola H, Kellomäki S. Comparison of two models for predicting the critical wind speeds required to damage coniferous trees. Ecological Modelling 2000;129(1):1-23. https://doi.org/https://doi.org/10.1016/S0304-3800(00)00220-9.
[22] Ryan HM. High Voltage Engineering and Testing. 2nd Edition ed.: Institution of Engineering and Technology; 2001
[23] Ansys Inc. LS-DYNA User Manual, Version 10.1.0. 2018.
[24] Priority Wire & Cable Inc. ACSR Cable Overview, https://www.prioritywire.com/acsr.php; 2024 [accessed 3/1/2024.
[25] National Wildfire Coordinating Group. Fire behavior field reference guide. PMS 437 ed.: Interagency Fire Center, Publication Management System; 2021.
[26] Andrews PL. The Rothermel surface fire spread model and associated developments: A comprehensive explanation. Gen Tech Rep RMRS-GTR-371 Fort Collins, CO: US Department of Agriculture, Forest Service, Rocky Mountain Research Station 121 p 2018;371.
[27] Scott JH. Standard fire behavior fuel models: a comprehensive set for use with Rothermel's surface fire spread model. US Department of Agriculture, Forest Service, Rocky Mountain Research Station; 2005
[28] Schaffer EL. Charring rate of selected woods--transverse to grain. US Department of Agriculture; 1967
[29] Glass S, Zelinka S. Moisture relations and physical properties of wood. Chapter 4 in FPL-GTR-282 2021:4-1-4-22.
[30] Weather Underground. Riverside, CA Weather History, https://www.wunderground.com/history/daily/us/ca/riverside/KRAL; 2024 3/1/2024].
[31] Bond ML, Lee DE, Bradley CM, Hanson CT. Influence of pre-fire tree mortality on fire severity in conifer forests of the San Bernardino Mountains, California. Open Forest Science Journal 2009;2:41-7.